DALTON
FULL PAPER

Syntheses, structures, magnetic, and spectroscopic properties of cobalt(II), nickel(II) and zinc(II) complexes containing 2-(6-methyl)pyridyl-substituted nitronyl and imino nitroxide †

Youhei Yamamoto, Takayoshi Suzuki and Sumio Kaizaki *

Department of Chemistry, Graduate School of Science, Osaka University, Toyonaka, Osaka, 560-0043, Japan. E-mail: kaizaki@chem.sci.osaka-u.ac.jp

Received 24th April 2001, Accepted 20th July 2001
First published as an Advance Article on the web 11th September 2001

Chelate complexation of 4,4,5,5-tetramethyl-2-(6-methyl-2-pyridyl)imidazolin-1-oxyl 3-oxide (NITmepy) and 4,4,5,5-tetramethyl-2-(6-methyl-2-pyridyl)imidazolin-1-oxyl (IMmepy) to cobalt(II) chloride (bromide) or zinc(II) chloride afforded tetrahedral four-co-ordinate (*T*-4) complexes, $[MX_2(NITmepy)]$ and $[MX_2(IMmepy)]$ (MX = CoCl (**1** and **2**), CoBr (**1Br** and **2Br**) or ZnCl (**3** and **4**), respectively) containing either a six- or a five-membered chelate ring as determined by single-crystal X-ray analysis. The formation of such *T*-4 complexes arises from the steric requirements of the methyl group at the *o*-position of the pyridyl-N donor. The UV-vis-NIR spectra suggest that both complexes **1** and **2** in dichloromethane retain their solid state structure. In acetonitrile, however, **1** exists as an equilibrium mixture due to dissociation of the co-ordinated NITmepy, while **2** is stable. The ligand-field spin-allowed and spin-forbidden d–d transitions of **1** and **2** are not influenced by the coordinated radical ligands. The reaction of nickel(II) chloride and thiocyanate with IMmepy gave a dichloro-bridged dinuclear complex with a square pyramidal five-co-ordinate (*SPR*-5) geometry and an *OC*-6 complex, respectively, $[\{NiCl(IMmepy)\}_2(\mu\text{-}Cl)_2]$ (**5**) and $[Ni(NCS)_2(IMmepy)_2]$ (**6**). The intramolecular magnetic interactions in **1** and **2** are estimated to be antiferromagnetic, whereas **5** and **6** give ferromagnetic interactions. Complex **3**, with one-dimensional columns, forms a dimer so that a moderate intermolecular antiferromagnetic coupling is demonstrated, while complex **4** exists as a discrete molecule in the crystal and shows paramagnetic behaviour.

Introduction

There has been a number of investigations concerning paramagnetic metal complexes with nitronyl nitroxide (NITR: 4,4,5,5-tetramethyl-2-R-imidazolin-1-oxyl 3-oxide) and imino nitroxide (IMR: 4,4,5,5-tetramethyl-2-R-imidazolin-1-oxyl) radicals in order to reveal the magnetic interactions between paramagnetic centres for the design of molecular-based ferromagnets.[1] Among them, the nitroxides substituted with pyridyl groups have the advantage of forming stable chelated complexes with the support of the auxiliary substituent groups.[2–5] However, there have been few reports on the magnetochemical influence on metal complexes containing such nitroxide chelates arising from the co-ordination geometry and/or co-ordination polyhedron around the metal ions. In the course of our recent studies on the spectroscopic properties in relation to the magnetism of NIT2py (4,4,5,5-tetramethyl-2-(2-pyridyl)imidazolin-1-oxyl 3-oxide) and IM2py (4,4,5,5-tetramethyl-2-(2-pyridyl)imidazolin-1-oxyl) transition metal complexes,[6–11] we have found a dependence of co-ordination geometry on the difference in the steric requirements of NIT2py and IM2py; stereospecific formation of *cis(Cl)-trans(py)*-$[MCl_2(IM2py)_2]$ and *trans(Cl)-trans(py)*-$[MCl_2(NIT2py)_2]$ ($M = Mn^{II}$, Co^{II}, Ni^{II} or Zn^{II}),[2,10,11] which is related to their magnetic and optical properties. On the other hand, the substitution of a methyl group at the *o*-position of the 2-pyridyl ring of the nitroxides is expected to result in the formation of tetrahedral four-co-ordinate (*T*-4) complexes instead of octahedral six-co-ordinate (*OC*-6) complexes associated with more severe steric crowding around the metal(II) centre. Such a steric requirement is inferred from the analogous reaction of cobalt(II) chloride with 6,6′-dimethyl-2,2′-bipyridyl (dmbpy) producing only a *T*-4 complex, $[CoCl_2(dmbpy)]$,[12] in contrast to the formation of the *OC*-6 complexes *cis*- and *trans*-$[CoCl_2(bpy)_2]$. Hence, we have examined the complexation reactions of NITmepy (4,4,5,5-tetramethyl-2-(6-methyl-2-pyridyl)imidazolin-1-oxyl 3-oxide) or IMmepy (4,4,5,5-tetramethyl-2-(6-methyl-2-pyridyl)imidazolin-1-oxyl) (Scheme 1) to cobalt(II) chloride or bromide, nickel(II) chloride or thiocyanate, or zinc(II) chloride. The products have been investigated from a magnetic and spectroscopic viewpoint on the basis of X-ray structure analyses. There have already been several reports on diamagnetic transition-metal complexes with NITmepy or IMmepy such as a mercury(II) complex with NITmepy by Lee *et al.*[3] and palladium(II), copper(I) and silver(I) complexes with IMmepy by Oshio *et al.*,[4,5] but none on paramagnetic metal(II) ions to the best of our knowledge.

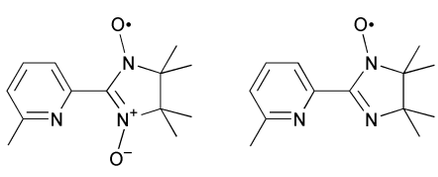

Scheme 1 The nitronyl and imino nitroxides.

† Electronic supplementary information (ESI) available: packing diagrams of complexes **1** and **2**, UV-vis-NIR absorption spectra of complexes **1** and **2** together with those of NITmepy and IMmepy, solvent-dependence of UV-vis absorption and MCD spectra of **1** in a mixture of dichloromethane and acetonitrile, temperature-dependence of the anisotropic magnetic properties for complex **1Br**. See http://www.rsc.org/suppdata/dt/b1/b103647p/

DOI: 10.1039/b103647p

Experimental

Preparations

The nitroxides, NITmepy and IMmepy, were prepared by methods similar to those for NIT2py and IM2py, respectively,[1,13] using 6-methylpyridine-2-aldehyde.

[$CoCl_2$(NITmepy)] (1), [$CoBr_2$(NITmepy)] (1Br), [$CoCl_2$(IMmepy)] (2) and [$CoBr_2$(IMmepy)] (2Br). An acetone solution (2 cm^3) containing $CoCl_2 \cdot 6H_2O$ (0.50 mmol) and NITmepy (0.50 mmol) was diffused with diethyl ether vapour in a desiccator at room temperature. The resulting dark green columnar crystals of [$CoCl_2$(NITmepy)] **1** were collected by filtration and dried in air (75%) (Found: C, 40.95; H, 4.74; N, 11.00. $C_{13}H_{18}Cl_2CoN_3O_2$ requires C, 41.29; H, 4.80; N, 11.11%; mp 168 °C). Dark green columnar crystals of [$CoBr_2$(NITmepy)] **1Br** were obtained by a similar method using $CoBr_2 \cdot 6H_2O$ (70%) (Found: C, 33.22; H, 3.83; N, 8.90. $C_{13}H_{18}Br_2CoN_3O_2$ requires C, 33.43; H, 3.88; N, 9.00%; mp 196 °C). Similarly with IMmepy dark red prismatic crystals of [$CoCl_2$(IMmepy)] **2** resulted (80%) (Found: C, 43.09; H, 4.88; N, 11.69. $C_{13}H_{18}Cl_2CoN_3O$ requires C, 43.12; H, 5.01; N, 11.60%; mp 219 °C) and [$CoBr_2$(IMmepy)] **2Br** were obtained (85%) (Found: C, 34.69; H, 3.94; N, 9.35. $C_{13}H_{18}Br_2CoN_3O$ requires C, 34.62; H, 4.02; N, 9.32%; mp 228 °C).

[$ZnCl_2$(NITmepy)] (3) and [$ZnCl_2$(IMmepy)] (4). To an acetone solution (3 cm^3) of $ZnCl_2$ (0.50 mmol) was added the respective nitroxide (0.50 mmol) with stirring, and the mixture was filtered to remove a small amount of precipitate. Diethyl ether vapour was diffused into the filtrate in a desiccator at room temperature. The deposited purple columnar crystals of [$ZnCl_2$(NITmepy)] **3** or red-orange prismatic crystals of [$ZnCl_2$(IMmepy)] **4** were collected by filtration and dried in air (**3**: 75%, Found: C, 40.27; H, 4.59; N, 10.85. $C_{13}H_{18}Cl_2N_3O_2Zn$ requires C, 40.60; H, 4.72; N, 10.93%; mp 170 °C. **4**: 80%, Found: C, 42.07; H, 4.86; N, 11.32. $C_{13}H_{18}Cl_2N_3OZn$ requires C, 42.36; H, 4.92; N, 11.40%; mp 203 °C).

[{NiCl(IMmepy)}$_2$(μ-Cl)$_2$] (5). A methanol solution (2 cm^3) containing $NiCl_2 \cdot 6H_2O$ (0.50 mmol) and IMmepy (0.50 mmol) was diffused with diethyl ether vapour in a desiccator at room temperature. Dark red plate crystals formed and were collected by filtration and dried in air (40%) (Found: C, 43.31; H, 4.95; N, 11.69. $C_{26}H_{36}Cl_4N_6Ni_2O_2$ requires C, 43.15; H, 5.01; N, 11.61%; mp 243 °C).

[Ni(NCS)$_2$(IMmepy)$_2$] (6). An aqueous nickel(II) thiocyanate solution (*ca.* 1.2 mol dm^{-3}) was prepared as follows: an aqueous solution (25 cm^3) of $Ba(NCS)_2$ (1.05 g, 3.6 mmol) was added with stirring to an aqueous solution (25 cm^3) of $NiSO_4 \cdot 6H_2O$ (0.98 g, 3.7 mmol), the immediately formed white precipitate of $BaSO_4$ was filtered off, and the filtrate was evaporated to 3 cm^3 under reduced pressure below 15 °C. Four drops (*ca.* 0.2 cm^3) of the aqueous nickel(II) thiocyanate solution were diluted with methanol (2 cm^3), and the solution was layered onto a dichloromethane solution (3 cm^3) of IMmepy (0.06 g, 0.26 mmol). The mixture was allowed to stand in a refrigerator for 4 d to give dark orange columnar crystals, which were collected by filtration and dried in air (40 %) (Found: C, 52.18; H, 5.58; N, 17.37. $C_{28}H_{36}N_8NiO_2S_2$ requires C, 52.59; H, 5.67; N, 17.52%; mp 195 °C).

Crystallography

The X-ray intensities were measured on a Rigaku automated four-circle diffractometer AFC-5R or AFC-7R (23 °C, graphite monochromated Mo-Kα radiation ($\lambda = 0.71073$ Å), ω–2θ scan mode, $2\theta_{max} = 60°$). The structures were solved by direct methods using the SHELXS-86 program[14] and refined on F^2 by full-matrix least-squares using SHELXL-97.[15] All calculations were carried out using the TeXsan software package.[16]

Crystal data are summarized in Table 1, selected structural parameters in Tables 2–5.

CCDC reference numbers 167810–167816.

See http://www.rsc.org/suppdata/dt/b1/b103647p/ for crystallographic data in CIF or other electronic format.

Measurements

The magnetic susceptibility data were collected with use of a SQUID-based sample magnetometer on a Quantum Design model MPMS instrument. Data were corrected for magnetization of the sample holder and for diamagnetic contributions, which were estimated from Pascal's constants. UV-vis spectra were measured on a Perkin-Elmer Lambda 19 spectrophotometer. Magnetic circular dichroism (MCD) spectra were recorded on a Jasco J-720W spectropolarimeter in a magnetic field of 1.5 T at room temperature.

Results and discussion

Syntheses and crystal structures of the complexes

Cobalt(II) and zinc(II) complexes. While reaction of $CoCl_2 \cdot 6H_2O$ with two equivalents of NIT2py or IM2py gave the 1 : 2 adducts [$CoCl_2$(NIT2py)$_2$]$\cdot 2CH_2Cl_2$[11] or [$CoCl_2$(IM2py)$_2$],[10] analogous reactions with NITmepy and IMmepy in acetone afforded dark green columnar crystals and dark red prismatic crystals, respectively, with chemical formulae for the 1 : 1 adducts of [$CoCl_2$(NITmepy)] **1** and [$CoCl_2$(IMmepy)] **2**. Reaction with an equivalent amount of the nitroxides gave 75–80% yields of the respective complexes. The corresponding dibromo complexes, [$CoBr_2$(NITmepy)] **1Br** or [$CoBr_2$(IMmepy)] **2Br** and the zinc(II) dichloro complexes, [$ZnCl_2$(NITmepy)] **3** or [$ZnCl_2$(IMmepy)] **4** were obtained similarly by using $CoBr_2 \cdot 6H_2O$ or $ZnCl_2$, respectively.

The molecular and crystal structures of the complexes except for **2Br** have been determined by single-crystal X-ray analysis. The NITmepy complexes of **1**, **1Br** and **3** are found to crystallize in an isomorphous monoclinic space group *Pn* with $Z = 4$, containing two crystallographically independent molecules. The two independent molecular structures of **1** are not significantly different from each other as shown in Fig. 1. The molecular structures of **1Br** are very similar to those of **1**. The complexes have a distorted *T*-4 geometry with two Cl (or Br) and a chelating NITmepy *via* the pyridyl-N and nitroxide-O atoms. The stereospecific formation of *T*-4 NITmepy complexes results in a reduction of the intramolecular steric crowding due to the methyl groups at the *o*-position of the pyridyl substituent in NITmepy, which is supposed to be severe for the hypothetical *OC*-6 bis(NITmepy) complexes. The average Zn–N bond length in **3** (2.101 Å) (Table 2) is slightly longer than those in the corresponding *T*-4 NIT2py complex [Zn–N = 2.080(3) Å],[11] while the Zn–O bond lengths in these NITmepy (average 2.037 Å) and NIT2py [2.031(3) Å][11] complexes are very similar. This difference in the Zn–N bond lengths may be also caused by the steric requirement of the methyl group in the pyridyl moiety.

The structural parameters of the co-ordinated NITmepy moiety in complexes **1** and **3** are comparable to those of the *OC*-6 NIT2py Co^{II} and Zn^{II} complexes.[11] The unco-ordinated N–O bonds [N(2)–O(2) and N(22)–O(22)] in NITmepy are shorter by *ca.* 0.03 Å than the co-ordinated N–O bonds [N(1)–O(1) and N(21)–O(21)]. The dihedral angle (*ca.* 34°) between the pyridyl plane and the nitronyl nitroxide plane in **1** and **3** is slightly larger than the corresponding angle (*ca.* 29°) in the *OC*-6 NIT2py complexes.[11] The bond angle (110–113°) of M–O–N (M = Co and Zn) and the torsion angle (absolute value of 42–50°) of M–O–N–C are slightly smaller and larger,

Table 1 Crystal data for the complexes

Compound	**1**	**1Br**	**2**	**3**	**4**	**5**	**6**
Formula	$C_{13}H_{18}Cl_2CoN_3O_2$	$C_{13}H_{18}Br_2CoN_3O_2$	$C_{13}H_{18}Cl_2CoN_3O$	$C_{13}H_{18}Cl_2N_3O_2Zn$	$C_{13}H_{18}Cl_2N_3OZn$	$C_{26}H_{36}Cl_4N_6Ni_2O_2$	$C_{28}H_{36}N_8NiO_2S_2$
M	378.13	467.05	362.13	384.57	368.57	723.82	639.48
Crystal system	Monoclinic	Monoclinic	Monoclinic	Monoclinic	Monoclinic	Monoclinic	Monoclinic
a/Å	7.361(3)	7.350(2)	15.613(2)	7.380(3)	15.667(1)	10.212(2)	11.904(4)
b/Å	19.112(2)	19.487(2)	13.236(2)	19.103(3)	13.265(2)	10.892(3)	17.073(3)
c/Å	11.851(2)	12.055(2)	15.866(3)	11.853(2)	15.885(2)	14.515(2)	15.216(2)
β/°	95.09(2)	95.49(2)	95.91(1)	95.74(2)	95.677(8)	99.29(1)	94.73(2)
U/Å^3	1660.7(6)	1718.6(5)	3261.2(8)	1662.6(8)	3285.2(7)	1593.3(5)	3082(1)
Space group	*Pn* (no. 7)	*Pn* (no. 7)	$P2_1/a$ (no. 14)	*Pn* (no. 7)	$P2_1/a$ (no. 14)	$P2_1/c$ (no. 14)	$P2_1/n$ (no. 14)
Z	4	4	8	4	8	2	4
μ(Mo-K$_\alpha$)/mm^{-1}	1.361	5.654	1.378	1.805	1.819	1.551	0.805
R_{int}	0.041	0.057	0.026	0.041	0.035	0.013	0.030
Reflns./param.	5203/387	5371/387	9507/371	5203/387	9577/371	4651/186	8983/380
$R1$ [$F^2 > 2\sigma(F^2)$]	0.038	0.043	0.040	0.034	0.043	0.030	0.044
wR (F^2 : all data)	0.110	0.128	0.114	0.099	0.128	0.085	0.128

respectively, than the corresponding angles in the NIT2py complexes.[2,11]

The crystal structures of **1**, **1Br** and **3** have stacking interactions between the intermolecular pyridine rings which form a one-dimensional column structure along the crystallographic *a* axis (see Fig. S1*a*) with two kinds of nonbonding intermolecular N–O···O–N distances in the column [O(2)···O(22) = 3.840(9) and O(22)···(2′) = 3.530(9) Å: see Fig. S1*b*]. This feature is important for the interpretation of the magnetic properties (*vide infra*).

The crystals of the IMmepy Co^{II} and Zn^{II} complexes **2** and **4** are found to be isomorphous: monoclinic space group $P2_1/a$ with $Z = 8$. The crystal and molecular structures of the Zn^{II} complex **4** are similar to those of the Co^{II} complex **2** having two independent molecules in the asymmetric unit, like the NITmepy complexes, as shown in Fig. 2. The molecules have a distorted *T*-4 geometry with two Cl and a chelated IMmepy *via* pyridyl-N and imino-N atoms. This co-ordination mode of IMmepy is similar to that of IM2py in *OC*-6 *cis(Cl)-trans(py)*-$[MCl_2(IM2py)_2]$.[10] As found in the bis(IM2py) complexes,[10] the imino nitroxide plane is almost coplanar to the pyridyl ring as well as to the planar chelate ring (Table 3).

For Co^{II} complex **2**, the average Co–N(im) bond length is relatively shorter by 0.09 Å than the average Co–N(py) one, in contrast to that for *cis(Cl)-trans(py)*-$[CoCl_2(IM2py)_2]$ where the Co–N(im) bond is longer by 0.04 Å than the Co–N(py) bond.[10] Such a reversal in bond lengths between M–N(im) and M–N(py) is seen for the Zn^{II} complexes **4** and *cis(Cl)-trans(py)*-$[ZnCl_2(IM2py)_2]$. It is also found that the Ni–N(py) bond of *cis(NCS)-trans(py)*-$[Ni(NCS)_2(IMmepy)_2]$ (*vide infra*) is remarkably elongated in comparison to that of *cis(Cl)-trans(py)*-$[NiCl_2(IM2py)_2]$[10] while the Ni–N(im) bonds in these complexes are similar.[2] Thus, it follows that the elongated M–N(py) bonds in the IMmepy complexes result from the steric disadvantage in co-ordinating the pyridyl-N donor due to the methyl group at the *o*-position of the pyridyl ring, independent of the coordination geometry (*T*-4 *versus OC*-6).

The crystal packing of the IMmepy complexes **2** and **4** is remarkably different from the NITmepy complexes (Fig. S2). There are no short intermolecular contacts between the imino nitroxide moieties; the shortest intermolecular distance is 4.779(4) Å for O(1)···N(1′). Hence, the IMmepy complex can be treated as a *discrete* molecule in the crystal.

Nickel(II) complexes containing IMmepy. Dark red plate crystals with the chemical composition $NiCl_2$(IMmepy) were obtained from the reaction of nickel(II) chloride hexahydrate with IMmepy in methanol. The X-ray analysis of this complex revealed that the Ni^{II} complex has a dinuclear structure bridged by two Cl ligands, $[\{NiCl(IMmepy)\}_2(\mu\text{-}Cl)_2]$ **5** (Fig. 3), in contrast to the above Co^{II} and Zn^{II} complexes. There is a crystallographic centre of symmetry at the midpoint of the two Ni atoms. The Ni···Ni′ distance is 3.5808(5) Å, indicative of the lack of a bonding interaction. The co-ordination geometry around the Ni centre is a square-based pyramid (*SPR*-5) with the imino-N atom at the apical position. The four basal sites are occupied by two bridging Cl, a terminal Cl and a pyridyl-N atom, and the Ni atom is displaced by 0.4312(5) Å above the mean basal plane. This geometrical structure would be the most favourable, because the methyl group at the *o*-position of the pyridyl ring is directed toward the most open space (void in Ψ-O_h) around the Ni co-ordination sphere. As mentioned above, the apical Ni–N(1) bond of the imino donor is shorter by 0.1 Å than the basal Ni–N(3) bond of the pyridyl donor (Table 4). The pyridyl ring and the imino nitroxide plane are found to be almost coplanar to each other. Irrespective of the different co-ordination geometry around the metal(II) centre, the structural characteristics of the IMmepy moiety of **5** are similar to those of **2** and **4**, and also *cis(Cl)-trans(py)*-$[NiCl_2(IM2py)_2]$.[10]

Table 2 Selected structural parameters (*l*/Å, *φ*/°) for complexes **1**, **1Br** and **3**

	1	**1Br**	**3**
M(1)–Cl(1)[*Br(1)*]	2.210(2)	*2.347(2)*	2.198(2)
M(2)–Cl(21)[*Br(21)*]	2.203(3)	*2.339(2)*	2.193(3)
M(1)–Cl(2)[*Br(2)*]	2.209(2)	*2.344(2)*	2.178(2)
M(2)–Cl(22)[*Br(22)*]	2.200(2)	*2.337(2)*	2.173(2)
M(1)–O(1)	1.977(4)	1.981(6)	2.034(3)
M(2)–O(21)	1.979(5)	1.981(7)	2.040(4)
M(1)–N(3)	2.070(5)	2.070(6)	2.091(4)
M(2)–N(23)	2.075(4)	2.067(7)	2.110(4)
O(1)–N(1)	1.303(5)	1.301(8)	1.305(5)
O(21)–N(21)	1.298(6)	1.302(9)	1.297(6)
O(2)–N(2)	1.268(6)	1.271(9)	1.259(6)
O(22)–N(22)	1.274(6)	1.29(1)	1.263(6)
O(1)–M(1)–N(3)	91.7(2)	91.7(2)	89.7(2)
O(21)–M(2)–N(23)	91.4(2)	91.9(3)	89.6(2)
Cl(1)[*Br(1)*]–M(1)–Cl(2)[*Br(2)*]	120.22(8)	*120.12(6)*	123.40(7)
Cl(21)[*Br(21)*]–M(2)–Cl(22)[*Br(22)*]	121.7(1)	*120.55(9)*	125.0(1)
M(1)–O(1)–N(1)–C(1)	−49.2(6)	−48.8(9)	−49.1(5)
M(2)–O(21)–N(21)–C(21)	44.2(7)	44(1)	45.4(6)
pl. $MCl_2(1)$[$MBr_2(1)$][a] *vs.* pl. MNO(1)[b]	71.87	*85.00*	86.83
pl. $MCl_2(2)$[$MBr_2(2)$][a] *vs.* pl. MNO(2)[b]	81.07	*79.94*	82.53
pl. MNO(1)[b] *vs.* pl. nit(1)[c]	51.7(3)	51.1(5)	52.3(3)
pl. MNO(2)[b] *vs.* pl. nit(2)[c]	49.6(3)	50.4(5)	51.1(3)
pl. MNO(1)[b] *vs.* pl. py(1)[d]	25.2(2)	25.2(2)	27.0(1)
pl. MNO(2)[b] *vs.* pl. py(2)[d]	24.9(1)	24.9(2)	26.9(1)
pl. nit(1)[c] *vs.* pl. py(1)[d]	34.3(2)	34.2(3)	34.6(2)
pl. nit(2)[c] *vs.* pl. py(2)[d]	33.7(2)	33.5(3)	34.6(2)

pl. = plane. [a] pl. $MCl_2(1)$[$MBr_2(1)$] defined by M(1), Cl(1)[*Br(1)*] and Cl(2)[*Br(2)*]; pl. $MCl_2(2)$ by M(2), Cl(21)[*Br(21)*] and Cl(22)[*Br(22)*]. [b] pl. MNO(1) defined by M(1), N(3) and O(1); pl. MNO(2) by M(2), N(23) and O(21). [c] pl. nit(1 or 2) denotes the least-square plane of the nitronyl nitroxide moiety. [d] pl. py(1 or 2) denotes the least-square plane of the pyridyl ring.

Table 3 Selected structural parameters (*l*/Å, *φ*/°) for complexes **2** and **4**

	2	**4**
M(1)–Cl(1)	2.212(1)	2.194(1)
M(2)–Cl(21)	2.203(1)	2.188(1)
M(1)–Cl(2)	2.215(1)	2.199(2)
M(2)–Cl(22)	2.223(1)	2.214(1)
M(1)–N(1)	1.985(3)	2.043(3)
M(2)–N(21)	1.990(3)	2.064(3)
M(1)–N(3)	2.075(3)	2.100(3)
M(2)–N(23)	2.075(2)	2.089(3)
O(1)–N(1)	1.257(3)	1.259(4)
O(21)–N(21)	1.256(3)	1.262(4)
N(1)–M(1)–N(3)	80.9(1)	79.4(1)
N(21)–M(2)–N(23)	80.9(1)	79.8(1)
Cl(1)–M(1)–Cl(2)	120.24(5)	122.87(6)
Cl(21)–M(2)–Cl(22)	113.17(4)	116.39(5)
M(1)–N(1)–C(1)–N(2)	177.4(2)	178.2(3)
M(2)–N(21)–C(21)–N(22)	176.2(2)	176.0(2)
pl. $MCl_2(1)$[a] *vs.* pl. $MN_2(1)$[b]	89.75	89.62
pl. $MCl_2(2)$[a] *vs.* pl. $MN_2(2)$[b]	89.89	89.40
pl. $MN_2(1)$[b] *vs.* pl. im(1)[c]	2.69(6)	2.10(9)
pl. $MN_2(2)$[b] *vs.* pl. im(2)[c]	6.01(9)	6.0(1)
pl. $MN_2(1)$[b] *vs.* pl. py(1)[d]	3.44(8)	3.7(1)
pl. $MN_2(2)$[b] *vs.* pl. py(2)[d]	4.36(8)	4.2(1)
pl. im(1)[c] *vs.* pl. py(1)[d]	0.7(1)	1.6(2)
pl. im(2)[c] *vs.* pl. py(2)[d]	5.1(2)	5.4(3)

pl. = plane. [a] pl. $MCl_2(1)$ defined by M(1), Cl(1) and Cl(2); pl. $MCl_2(2)$ by M(2), Cl(21) and Cl(22). [b] pl. $MN_2(1)$ defined by M(1), N(1) and N(3); pl. $MN_2(2)$ by M(2), N(21) and N(23). [c] pl. im(1 or 2) denotes the least-square plane of the imino nitroxide moiety. [d] pl. py(1 or 2) denotes the least-square plane of the pyridyl ring.

We have obtained a powder for the corresponding NITmepy Ni^{II} complex with composition $NiCl_2$(NITmepy); a single-crystal suitable for X-ray analysis could not be grown.

With the expectation of forming a *T*-4 thiocyanate complex analogous to **2** and **4** due to the poorer bridging ability of thiocyanate, preparation of the thiocyanato nickel(II) complex with IMmepy has also been attempted. However, the X-ray analysis demonstrated that the product isolated from a 1 : 1 mixture of nickel(II) thiocyanate and IMmepy in 40% yield is an *OC*-6 bis(IMmepy) complex, *cis(NCS)-trans(py)*-[$Ni(NCS)_2$-$(IMmepy)_2$] **6** (Fig. 4). The remarkably long Ni–N(py) bond lengths and nonplanarity between the pyridine ring and the imino nitroxide plane in **6** (Table 5) result from the steric requirement for *OC*-6 co-ordination as compared with that of the corresponding *cis(Cl)-trans(py)*-[$MCl_2(IM2py)_2$][10] and/or **2**, **4**, **5** for *T*-4/*SPR*-5.

Table 4 Selected structural parameters (*l*/Å, *φ*/°) for complex **5**

Ni · · · Ni′	3.5808(5)	Ni–Cl(1)	2.2820(6)
Ni–Cl(2)	2.3554(7)	Ni–Cl(2′)	2.4197(8)
Ni–N(1)	2.002(2)	Ni–N(3)	2.103(2)
N(2)–O(1)	1.262(2)		
pl. NiN_2[a] *vs.* pl. im[b]	5.36(8)	N(1)–Ni–N(3)	79.78(6)
pl. NiN_2[a] *vs.* pl. py[c]	5.19(5)	Ni–Cl(2)–Ni′	97.15(2)
pl. im[b] *vs.* pl. py[c]	4.4(2)	Cl(2)–Ni–Cl(2′)	82.85(2)
		Ni–N(1)–C(1)–N(2)	−174.1(1)

pl. = plane. [a] pl. NiN_2 defined by Ni, N(1) and N(3). [b] pl. im denotes the least-square plane of the imino nitroxide moiety. [c] pl. py denotes the least-square plane of the pyridyl ring.

Solution structures and spectroscopic properties of the cobalt(II) complexes

As inferred from the similarity between the absorption spectra in the solid and in dichloromethane, the *T*-4 co-ordination of the NITmepy and IMmepy complexes in the crystals is retained in dichloromethane. Since the UV-vis spectrum of **1** shows a clear solvent-dependence with increasing acetonitrile ratio in a mixture of dichloromethane and acetonitrile (Fig. S3), there seems to be an equilibrium associated with the dissociation of NITmepy from [$CoCl_2$(NITmepy)].

It can be seen (from Fig. S4) that the second d–d $^4A_2 \longrightarrow {}^4T_{1a}$ and third $^4A_2 \longrightarrow {}^4T_{1b}$ band components are not so much affected by co-ordination of NITmepy as are the analogous Ni^{II} complexes,[7] since the absorption bands at 7350 and 9570 cm^{-1} for **1** in dichloromethane are similar to those of $[CoCl_4]^{2-}$ and the

Table 5 Selected structural parameters (*l*/Å, *φ*/°) for complex **6**

Ni–N(1)	2.133(2)	Ni–N(21)	2.115(2)
Ni–N(3)	2.242(2)	Ni–N(23)	2.218(2)
Ni–N(41)	2.023(2)	Ni–N(42)	2.030(2)
N(2)–O(1)	1.270(3)	N(22)–O(21)	1.271(3)
N(41)–C(41)	1.152(3)	N(42)–C(42)	1.145(4)
C(41)–S(1)	1.625(3)	C(42)–S(2)	1.630(3)
N(1)–Ni–N(3)	77.78(8)	N(21)–Ni–N(23)	77.40(8)
Ni–N(41)–C(41)	164.5(3)	Ni–N(42)–C(42)	174.9(3)
N(41)–C(41)–S(1)	179.4(3)	N(42)–C(42)–S(2)	178.9(3)
Ni–N(1)–C(1)–N(2)	−169.1(2)	Ni–N(21)–C(21)–N(22)	−177.8(2)
pl. $NiN_2(1)^a$ *vs.* pl. im(1)^b	10.2(2)	pl. $NiN_2(2)^a$ *vs.* pl. im(2)^b	8.4(2)
pl. $NiN_2(1)^a$ *vs.* pl. py(1)^c	4.22(7)	pl. $NiN_2(2)^a$ *vs.* pl. py(2)^c	15.95(8)
pl. im(1)^b *vs.* pl. py(1)^c	12.4(1)	pl. im(2)^b *vs.* pl. py(2)^c	16.0(2)

pl. = plane. [a] pl. $NiN_2(1)$ defined by Ni, N(1) and N(3); $NiN_2(2)$ by Ni, N(21) and N(23). [b] pl. im(1 or 2) denotes the least-square plane of the imino nitroxide moiety. [c] pl. py(1 or 2) denotes the least-square plane of the pyridyl ring.

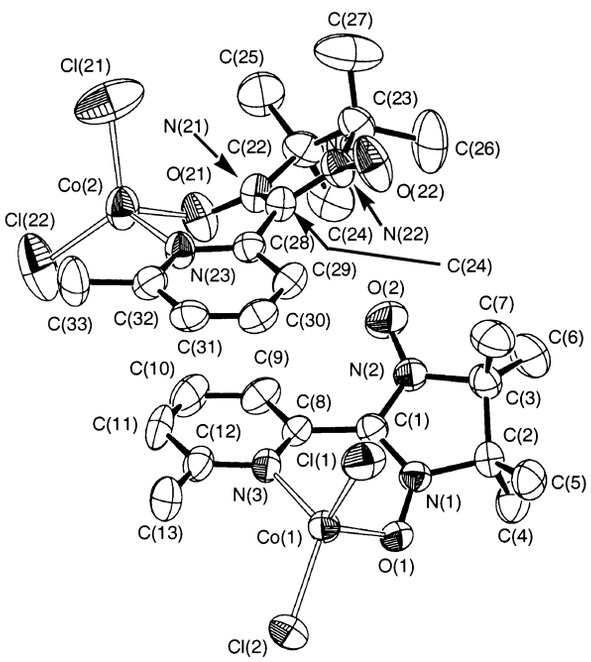

Fig. 1 Perspective drawings of two crystallographically independent molecules in $[CoCl_2(NITmepy)]$ **1**. Hydrogen atoms are omitted for clarity, and the thermal elipsoids are drawn at 50% probability level.

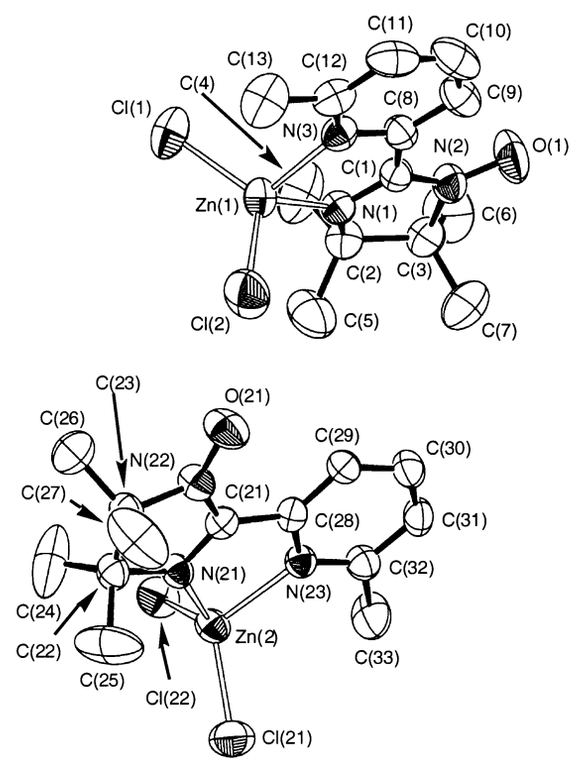

Fig. 2 Perspective drawings of two crystallographically independent molecules in $[ZnCl_2(IMmepy)]$ **4**. Hydrogen atoms are omitted for clarity, and the thermal elipsoids are drawn at 50% probability level.

three absorption maxima (15080, 16310 and 17510 cm^{-1}) of complex **1** are close to those (14800, 16400 and 17530 cm^{-1}) of $CoCl_2{\cdot}6H_2O$ in acetonitrile. This is also supported by the negligible solvent-dependent change at 15000–20000 cm^{-1} of the MCD spectrum of **1** in a mixture of dichloromethane and acetonitrile (Fig. S3).

In contrast to the NITmepy complex **1**, the absorption spectra of the IMmepy complex **2** in dichloromethane or acetonitrile coincide with each other, and are similar to the UV-vis spectrum in the solid state. These facts indicate that the co-ordination of IMmepy to the Co^{II} centre is also maintained in acetonitrile, indicative of the stronger co-ordination ability of the imino-N donor of IMmepy with a five-membered chelate than the nitroxide-O donor of NITmepy with a six-membered chelate.

In complex **2** in dichloromethane, the high energy component at 7850 cm^{-1} in the $^4A_2 \longrightarrow {}^4T_{1a}$ transition (Fig. S5) is located at higher frequency than the corresponding transition at 7350 cm^{-1} for **1**. Thus, the ligand-field perturbation of IMmepy *via* the imino-N donor is stronger than NITmepy *via* the nitroxide-O donor as expected from comparison of their stability in acetonitrile (*vide supra*) and in terms of the spectrochemical series.

The influence of the co-ordinated NITmepy and IMmepy ligands on the spin-forbidden $^4A_2 \longrightarrow {}^2E$, $^2T_1$ transitions was also noted. In view of the chelating co-ordination of the radical ligand in these Co^{II} complexes, a notable influence on the spin-forbidden transition intensity in the spin-coupled systems for transition metal complexes with dinuclear structures is expected;[17] a similar influence on the radical ligands such as the mono- and bis(NIT2py or IM2py)nickel(II) complexes and mono(NIT2py)chromium(III) complexes is also expected.[6,7,9–11] However, the spectral patterns of the spin-forbidden transitions overlapped with the third $^4A_2 \longrightarrow {}^4T_{1b}$ transitions are similar to those of the non-radical *T*-4 Co^{II} complexes, and the molar absorption coefficients are unchanged on radical co-ordination. The MCD pattern in this region is also not very different in its position and intensity from the non-radical Co^{II} complexes.[18] Some parts of the observed vibronic structures or "dips" are considered to result from the so-called antiresonance effect for the nearly degenerate location of the doublet ^2E,$^2T_1$ and quartet $^4T_{1b}$ states between which mixing occurs by spin–orbit coupling.[19] The sharp components in the spin-forbidden transformations do not always intensify with increasing observed magnetic interaction constants (*J*) estimated from the magnetic susceptibility.[7,9] Therefore it is not necessarily unreasonable that

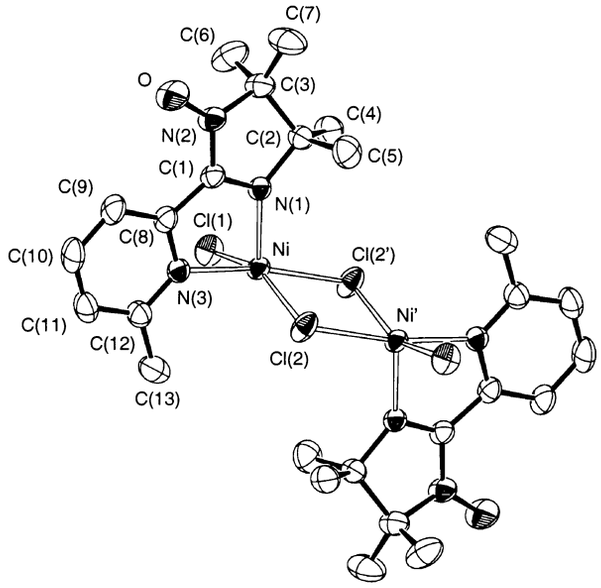

Fig. 3 Perspective drawings of $[\{NiCl(IMmepy)\}_2(\mu\text{-}Cl)_2]$ **5**. Hydrogen atoms are omitted for clarity, and the thermal elipsoids are drawn at 50% probability level.

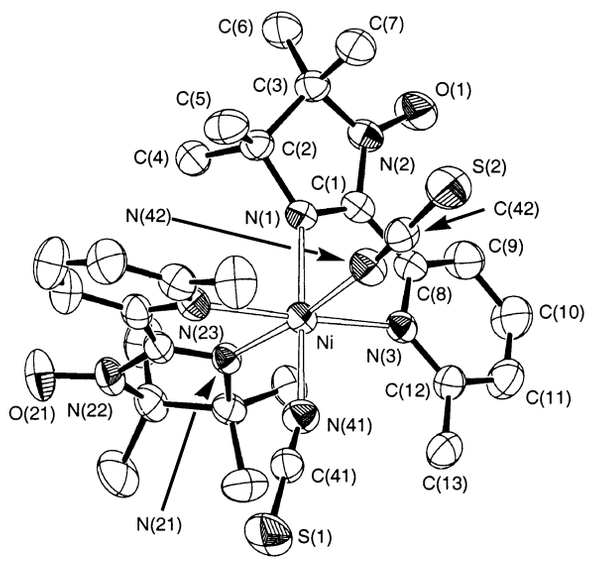

Fig. 4 Perspective drawings of *cis(NCS)-trans(py)*-$[Ni(NCS)_2(IMmepy)_2]$ **6**. Hydrogen atoms are omitted for clarity, and the thermal elipsoids are drawn at 50% probability level.

the intensity enhancement due to radical co-ordination is apparently very small for the present T-4 NITmepy and IMmepy Co^{II} complexes even though the observed antiferromagnetic interactions could be considerable (*vide infra*). In general, the spin-forbidden transition intensity enhancement may be explained in terms of the exchange mechanism, where the intensity borrows from the CT intensity by mixing with the CT through the electron transfer integral. Thus, the extent of the intensity enhancement depends on the CT transition energy and intensity as well as the antiferromagnetic interaction in the ground state.[7,9,17] No appreciable enhancement of the IMmepy and NITmepy complexes arises from the high energy position and low intensity of the CT concerned, though the CT position and intensity are not clearly identified so far.

Magnetic properties

Zinc(II) complexes. The temperature-dependence of the molar magnetic susceptibility (χ_M) and $\chi_M T$ for $[ZnCl_2(NITmepy)]$ **3** are shown in Fig. 5*a*, and those of $\chi_M T$ and χ_M^{-1} for $[ZnCl_2(IMmepy)]$ **4** in Fig. 5*b*. For both complexes, the

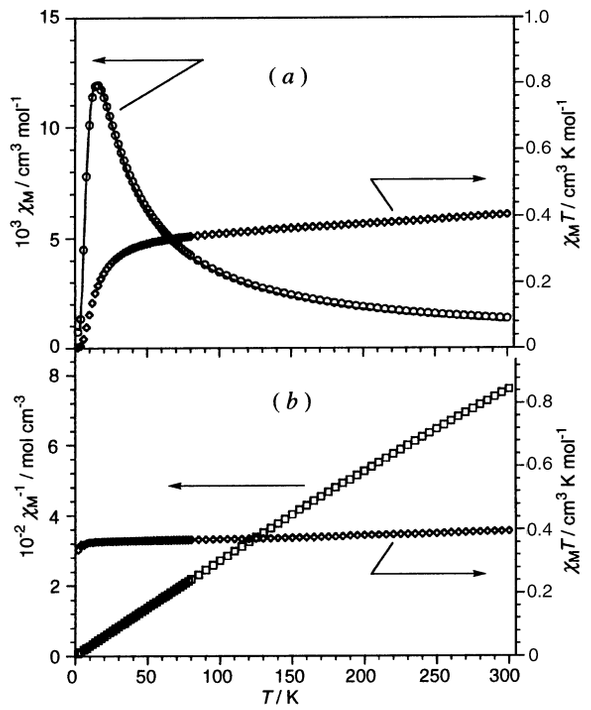

Fig. 5 Temperature-dependence of the magnetic properties (*a*) for complex **3** in the form of χ_M *vs.* T and $\chi_M T$ *vs.* T and (*b*) for complex **4** in the form of $\chi_M T$ *vs.* T and χ_M^{-1} *vs.* T. The solid line in (*a*) represents the best-fit calculation data.

observed $\chi_M T$ at 300 K is close to the expected value for an uncorrelated $S = 1/2$ spin (0.375 cm^3 K mol^{-1}). However, at lower temperatures the behaviour of the magnetic properties of two compounds are remarkably different from each other. The IMmepy complex **4** shows typical paramagnetic behaviour: $\chi_M T$ is almost temperature independent. This illustrates that complex **4** exists as a magnetically discrete molecule in the crystal, as found in the crystal structure analysis. The χ_M^{-1} *versus* T plot gives a Weiss temperature θ of $-0.426(4)$ K ($g = 1.983(1)$), indicating very weak intermolecular antiferromagnetic interactions.

In contrast, the NITmepy complex **3** shows a remarkable decrease in $\chi_M T$ below 50 K, which tends to zero at the lowest temperature. This indicates that moderate intermolecular antiferromagnetic interactions exist. Since the crystal structure of **3** showed a stacked column structure with two kinds of close contact between the intermolecular nitronyl nitroxide moieties, the temperature-dependence of χ_M was analyzed as an alternative chain model ($2J$ and $2\alpha J$ are the coupling constants in the chain).[20] The molecular field approximation was used for the interchain interaction. The resultant $2J$ and α values are $-17.85(6)$ cm^{-1} and 0.021(2), respectively, and the g value and the Weiss temperature are found to be $g = 2.013(2)$ and $\theta = -0.64(4)$ K. The negligibly small α value indicates that in the crystal complex **3** can be treated magnetically as a dimer.

Cobalt(II) complexes with IMmepy. The temperature-dependence of χ_M and $\chi_M T$ for the powdered samples of $[CoCl_2(IMmepy)]$ **2** and $[CoBr_2(IMmepy)]$ **2Br** are shown in Fig. 6. Both complexes show a similar behaviour for the $\chi_M T$ *versus* T plot. On cooling, $\chi_M T$ ($\approx$1.75 cm^3 K mol^{-1} at 300 K) decreases slightly to give a plateau around 150 K, where the $\chi_M T$ value is $\approx$1.4 and $\approx$1.55 cm^3 K mol^{-1} for complexes **2** and **2Br**, respectively. This behaviour can be accounted for by a strong intramolecular antiferromagnetic coupling between high-spin Co^{II} ($S_{Co} = 3/2$) and IMmepy ($S_R = 1/2$). Below 50 K, the $\chi_M T$ value decreases markedly, closing to zero at the lowest temperature. Since the crystal structure of **2** is found to be isomorphous with the Zn^{II} analogue **4**, it is expected that the

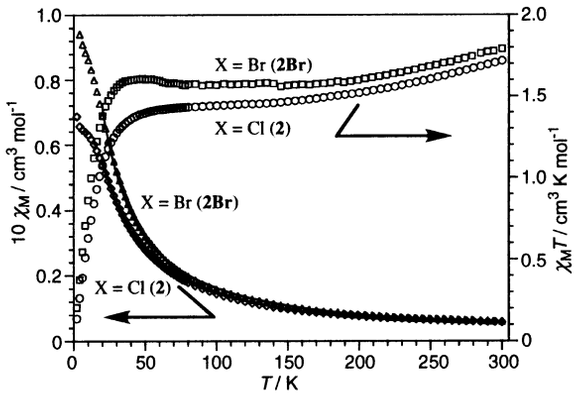

Fig. 6 Temperature-dependence of the magnetic properties for complexes **2** and **2Br** in the form of χ_M *vs.* T and $\chi_M T$ *vs.* T.

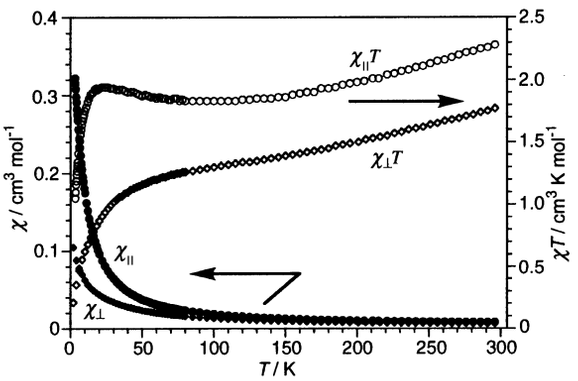

Fig. 7 Temperature-dependence of the anisotropic magnetic properties for complex **1** in the form of $\chi_{(\parallel \text{ or } \perp)}$ *vs.* T and $\chi_{(\parallel \text{ or } \perp)}T$ *vs.* T. $\chi_{\parallel}$ denotes the molar magnetic susceptibility when the crystallographic *a* axis is parallel to the magnetic field, and $\chi_{\perp}$ denotes that when the *a* axis is directed perpendicular to the magnetic field.

intermolecular magnetic coupling is too small to cause such a marked decrease in $\chi_M T$ below 50 K. Therefore, a significant zero-field splitting of the antiferromagnetically coupled $S = 1$ ground state is presumed. Under such conditions, the temperature variation of χ_M was analyzed. In the fitting process, the parameters g_R (1.983) and θ (−0.426 K) derived from the analysis of the Zn^{II} analogue **4** were used. No set of parameters for g_{Co}, J, and the zero-field splitting parameter $|D|$ could reproduce the χ_M behaviour below 10 K. This is because the intermolecular interactions of complexes **2** and **2Br** might be larger than the assumed value in view of the existence of spin density on the Co^{II} centre. Therefore, only the observed data above 20 K were used in the analysis. The best-fit parameters obtained are: $g_{Co} = 2.336(1)$, $J = -144(2)$ cm^{-1} and $|D| = 31.9(1)$ cm^{-1} for complex **2**: $g_{Co} = 2.442(4)$, $J = -195(26)$ cm^{-1} and $|D| = 21.4(5)$ cm^{-1} for complex **2Br**. Since the obtained g_{Co} and $|D|$ values are considered to be acceptable in view of the corresponding parameters of the other tetrahedral Co^{II} complexes concerned,[21] it can be concluded that the magnetic coupling between Co^{II} and IMmepy is largely antiferromagnetic.

Cobalt(II) NITmepy complexes. The magnetic properties of the Co^{II}–NITmepy complexes **1** and **1Br**, isomorphous to the Zn^{II} analogue **3**, are treated as a dimer (4 spin system) with a rather large zero-field splitting of the Co^{II} centre, similar to the above Co^{II}–IMmepy complexes. The complex analysis of such a multi-spin system may be made feasible by the measurement of the magnetic anisotropy of a suitable single-crystal. Fig. 7 shows the temperature-dependence of $\chi_{(\parallel \text{ or } \perp)}$ and $\chi_{(\parallel \text{ or } \perp)}T$ of a single-crystal of complex **1**, where the crystallographic *a* axis along the direction of the columnar structure is parallel or perpendicular to the magnetic field. $\chi_{\parallel}T$ shows a gradual decrease followed by a plateau around 150 K and a slight increase with a

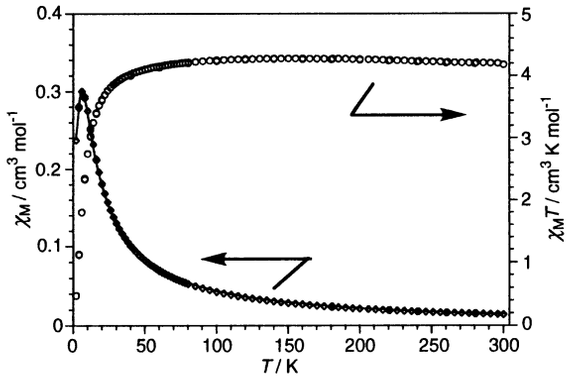

Fig. 8 Temperature-dependence of the magnetic properties for complex **5** in the form of χ_M *vs.* T and $\chi_M T$ *vs.* T. The solid line represents the best-fit calculation data (see text).

maximum up to 25 K and a sharp final decrease on cooling. In contrast, $\chi_{\perp}T$ indicates a monotonous decrease to *ca.* 50 K and then a deeper decrease tending to zero. The corresponding plots for complex **1Br** (Fig. S5) show similar behavour. These anisotropic magnetic exchange interactions suggest a negative axial zero-field splitting parameter D in the Co^{II}–NITmepy complexes. The average magnetic susceptibilities approximated by $\chi_M = 1/3\ \chi_{\parallel} + 2/3\ \chi_{\perp}$ for both complexes **1** and **1Br** coincide well with the observed ones for the powdered samples, and fairly well with those of complexes **2** and **2Br**. Thus, both the intramolecular Co^{II}–NITmepy and the intermolecular NITmepy–NITmepy interactions seem to be antiferromagnetic, although it is difficult to parameterize their interactions at present.

[{NiCl(IMmepy)}$_2$(μ-Cl)$_2$]. $\chi_M T$ of the dichloro-bridged dinuclear Ni^{II} complex **5** at 300 K is much higher than the value expected for the non-interacting two $S_{Ni} = 1$ and two $S_R = 1/2$ spins system. On lowering the temperature, $\chi_M T$ increases slightly to reach a plateau at 200–120 K (Fig. 8). This suggests that the interaction between Ni^{II} and IMmepy in each NiCl(IMmepy) moiety is strongly ferromagnetic, similar to the bis(IMmepy) (*vide infra*) and the analogous bis(IM2py) complexes.[2,10] A two step decrease, gradual below 150 K and sharp below 20 K, of $\chi_M T$ may be responsible for either one of the intra- and inter-molecular antiferromagnetic interactions or the zero-field splitting of the ground quartet state of the NiCl(IMmepy) moieties and/or a combination. Such a complicated analysis of the magnetic properties of complex **5** with a four-spin system may be made possible by applying the method used for a dichloro-bridged dinuclear Mn^{II} complex with nitronyl nitroxide-substituted phosphine oxide (*o*PONit = 2-(4,4,5,5-tetramethylimidazolin-2-yl-1-oxyl 3-oxide)phenyldiphenylphosphine oxide), [{MnCl(*o*PONit)}$_2$(μ-Cl)$_2$][22] which was expected to have a strong Mn^{II}–*o*PONit antiferromagentic and a rather weak ferromagnetic interaction J' ($|J_{Mn\text{–}R}| >> |J'|$) between two Mn^{II}–*o*PONit moieties with an effective $S = 2$ unit. As a result of the analysis of the temperature-dependence of χ_M of complex **5** (Fig. 8) using an antiferromagnetic interaction parameter J' between two $S = 3/2$ effective spin units (Ni^{II}–IMmepy), the following parameters are estimated: $g = 2.121(4)$, $2J_{Ni\text{–}R} = 200(5)$ cm^{-1}, $2J' = -130(2)$ cm^{-1} and $\theta = -1.88(6)$ K. The g and $J_{Ni\text{–}R}$ values are reasonable, but J' is too large for the assumption $|J_{Ni\text{–}R}| >> |J'|$. Irrespective of the estimated large negative Weiss temperature, a remarkable decrease of $\chi_M T$ below 20 K seems to result from the zero-field splitting of the ground quartet state of NiCl(IMmepy) in view of no close contacts between the neighbouring imino nitroxide moieties in the crystal structure (*vide supra*).

[Ni(NCS)$_2$(IMmepy)$_2$]. The temperature-dependence of χ_M and $\chi_M T$ of *OC*-6-*cis(NCS)-trans(py)*-[Ni(NCS)$_2$(IMmepy)$_2$]

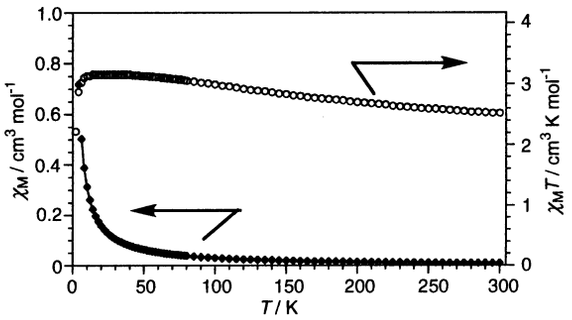

Fig. 9 Temperature-dependence of the magnetic properties for complex **6** in the form of χ_M *vs.* T and $\chi_M T$ *vs.* T. The solid line represents the best-fit calculation data (see text).

6 are shown in Fig. 9. $\chi_M T$ at 300 K is larger than the expected value for an independent spin ($S_{Ni} = 1$ and two $S_R = 1/2$) system. Since $\chi_M T$ gradually increases to give a plateau at 50 K with the $\chi_M T$ value of 3.15 cm^3 K mol^{-1} for the $S = 2$ ground state, there is a ferromagnetic interaction between the Ni^{II} dσ and IMmepy SOMO π^* magnetic orbitals. Further cooling from 5 K gives a sharp decrease of $\chi_M T$, showing either the intermolecular antiferromagnetic coupling or the zero-field splitting of the ground quintet state. According to the procedure applied to the similar magnetic behaviour of the anagolous Ni^{II}–IM2py complex, *OC*-6-*cis(Cl)-trans(py)*-[NiCl$_2$(IM2py)$_2$] with a fairly large ferromagnetic interaction with use of the intramolecular IMmepy–IMmepy magnetic interaction parameter ($2J' = -19$ cm^{-1}) for the bis(IMpy) Zn^{II} complex,[10] the best fit parameters are estimated to be $g_{Ni} = 2.142(3)$, $2J = 134(3)$ cm^{-1}, and $\theta = -0.37(1)$ K (g_R was set to be 2). The ferromagnetic interaction between Ni^{II} and IMmepy in **6** is as large as that of the bis(IM2py) Ni^{II} complex, which is consistent with the similar co-ordination structures of the complexes, as found in the X-ray analysis (*vide supra* and Table 5).

Concluding remarks

Introduction of a methyl group at the *o*-position of the pyridyl-N donor of nitronyl/imino nitroxide results in the stereospecific formation of the NITmepy and IMmepy complexes: (*T*-4)-[MCl$_2$(NITmepy)] and (*T*-4)-[MCl$_2$(IMmepy)] (M = Co^{II} and Zn^{II}); owing to the steric requirements of the methyl group. Reaction of NiCl$_2$ or Ni(NCS)$_2$ with IMmepy affords a dichloro-bridged dinuclear *SPR*-5 or mononuclear *OC*-6 complex. The ligand-field spin-forbidden d–d transitions in the UV region of (*T*-4)-[CoCl$_2$(IMmepy)] are not apparently influenced by the radical co-ordination unlike the case of the *OC*-6 NIT2py–Ni^{II} complexes which exhibit an intensity enhancement in their spin-forbidden transitions.

The magnetic properties of the Co^{II}–NITmepy, Zn^{II}–NITmepy complexes and the corresponding IMmepy complexes can be accounted for by assuming a dimer in a one-dimensional stacked columnar structure and a discrete molecule, respectively. The interactions of tetrahedral Co^{II} with NITmepy and with IMmepy are found to be antiferromagnetic, but those of square-pyramidal Ni^{II} with IMmepy and octahedral Ni^{II} with IMmepy are both found to be ferromagnetic. Irrespective of the introduction of the methyl group and the difference in co-ligands around the Ni^{II} centre, the magnetic interaction parameters between Ni^{II} and IMmepy (IM2py) are nearly the same in *cis(NCS)-trans(py)*-[Ni(NCS)$_2$(IMmepy)$_2$] and *cis(Cl)-trans(py)*-[NiCl$_2$(IM2py)$_2$].

Acknowledgements

We gratefully acknowledge support of this research by a Grant-in-Aid for Scientific Research (No. 10304056) from the Ministry of Education, Science and Culture.

References

1 (*a*) A. Caneschi, D. Gatteschi and P. Rey, *Prog. Inorg. Chem.*, 1991, **39**, 331 and references therein; (*b*) O. Kahn, *Molecular Magnetism*, VCH, New York, 1993; (*c*) E. Coronado, P. Dellhaès, D. Gatteschi and J. S. Miller (Editors), *Molecular Magnetism: From Molecular Assemblies to the Decives*, NATO ASI Series 321, Kluwer Academic Publishers, Dordrecht, 1996.
2 D. Luneau, G. Risoan, P. Rey, A. Grand, A. Caneschi, D. Gatteschi and J. Laugier, *Inorg. Chem.*, 1993, **32**, 5616.
3 C.-J. Lee, C.-H. Huang, H.-H. Wei, Y.-H. Liu, G.-H. Lee and Y. Wang, *J. Chem. Soc., Dalton Trans.*, 1998, 171.
4 (*a*) H. Oshio, T. Watanabe, A. Ohto, T. Ito and U. Nagashima, *Angew. Chem., Int. Ed. Engl.*, 1994, **33**, 670; (*b*) H. Oshio, T. Watanabe, A. Ohto, T. Ito and H. Masuda, *Inorg. Chem.*, 1996, **35**, 472; (*c*) H. Oshio, T. Watanabe, A. Ohto, T. Ito, T. Ikoma and S. Tero-Kubota, *Inorg. Chem.*, 1997, **36**, 3014.
5 H. Oshio, A. Ohto and T. Ito, *Chem. Commun.*, 1996, 1541.
6 T. Yoshida, K. Kanamori, S. Takamizawa, W. Mori and S. Kaizaki, *Chem. Lett.*, 1997, 603.
7 T. Yoshida, T. Suzuki, K. Kanamori and S. Kaizaki, *Inorg. Chem.*, 1999, **38**, 1059.
8 T. Yoshida and S. Kaizaki, *Inorg. Chem.*, 1999, **38**, 1054.
9 Y. Tsukahara, T. Yoshida, A. Iino, T. Suzuki and S. Kaizaki, to be submitted.
10 Y. Yamamoto, T. Suzuki and S. Kaizaki, *J. Chem. Soc., Dalton Trans.*, 2001, 1566.
11 Y. Yamamoto, T. Yoshida, T. Suzuki and S. Kaizaki, *Inorg. Chim. Acta*, in press.
12 G. L. Baker, F. R. Fronczek, G. E. Kiefer, C. R. Marston, C. L. Modenbach, G. R. Newkome, W. E. Puckett and S. F. Watkins, *Acta Crystallogr., Sect. C*, 1988, **44**, 1668.
13 (*a*) T. Akita, Y. Yazaki, K. Kobayashi, N. Koga and H. Iwamura, *J. Org. Chem.*, 1995, **60**, 2092; (*b*) E. F. Ullman, J. H. Osiecki, D. G. B. Boocock and R. Darcy, *J. Am. Chem. Soc.*, 1974, **94**, 7049; (*c*) E. F. Ullman, L. Call and J. H. Osiecki, *J. Org. Chem.*, 1970, **35**, 3623.
14 G. M. Sheldrick, *Acta Crystallogr., Sect. A*, 1990, **46**, 467.
15 G. M. Sheldrick, SHELXL-97, University of Göttingen, Germany, 1997.
16 TeXsan, Single Crystal Structure Analysis Software, ver. 1.10, Molecular Structure Corp., The Woodlands, TX, USA and Rigaku Co. Ltd., Akishima, Tokyo, Japan, 1999.
17 (*a*) P. J. McCarthy and H. U. Güdel, *Coord. Chem. Rev.*, 1988, **88**, 69; (*b*) C. Cador, C. Mathonieres and O. Kahn, *Inorg. Chem.*, 2000, **39**, 3799.
18 T. A. Kaden, B. Holmouist and B. Vallee, *Inorg. Chem.*, 1974, **13**, 2585.
19 (*a*) P. J. McCarthy and M. T. Vala, *Mol. Phys.*, 1973, **25**, 17; (*b*) M. D. Sturge, *J. Chem. Phys.*, 1969, **51**, 1254; (*c*) M. D. Sturge, H. J. Guggenheim and M. H. L. Pryce, *Phys. Rev.*, 1970, **B2**, 2459; (*d*) C. J. Ballhausen, *J. Pure Appl. Chem.*, 1975, **44**, 13.
20 O. Kahn, *Molecular Magnetism*, VCH, New York, 1993, ch. 11.
21 D. B. Brown, V. H. Crawford, J. W. Hall and W. E. Hatfield, *J. Phys. Chem.*, 1977, **81**, 1303.
22 C. Rancurel, D. B. Leznoff, J.-P. Sutter, P. Guionneau, D. Chasseau, J. Kliava and O. Kahn, *Inorg. Chem.*, 2000, **39**, 1602.